

南天山洋古生代期间俯冲作用过程探讨*

张斌¹ 陈文^{1**} 喻顺¹ 尹继元¹ 李洁¹ 孙敬博¹ 杨莉^{1,2} 杨静¹

ZHANG Bin¹, CHEN Wen^{1**}, YU Shun¹, YIN JiYuan¹, LI Jie¹, SUN JingBo¹, YANG Li^{1,2} and YANG Jing¹

1. 中国地质科学院地质研究所同位素热年代学实验室, 大陆构造与动力学国家重点实验室, 北京 100037

2. 昆明理工大学, 昆明 650093

1. State Key Laboratory of Continental Tectonics and Dynamics; Laboratory of Isotope Thermochronology, Institute of Geology, Chinese Academy of Geological Sciences, Beijing 100037, China

2. Kunming University of Science and Technology, Kunming 650093, China

2014-02-10 收稿, 2014-05-16 改回.

Zhang B, Chen W, Yu S, Yin JY, Li J, Sun JB, Yang L and Yang J. 2014. Subduction process of South Tianshan Ocean during Paleozoic. *Acta Petrologica Sinica*, 30(8):2351–2362

Abstract The subduction process of South Tianshan Ocean is a significance aspect of Central-Asian Orogenic Belt research and there still exists a controversy concerning the way of subduction. A series of nearly east-west distribution of intermediate-acid intrusive rocks are exposed in southern margin of the South Tianshan and selected as the object of this research. Ouxidaban quartz diorite, located in the region, i. e. the north of Kuqa foreland basin, is studied in detail in this paper. Geochemical characteristics suggest that Ouxidaban quartz diorite has SiO₂ (54.23% ~ 56.27%), Al₂O₃ (15.15% ~ 16.03%), CaO (6.44% ~ 7.56%), K₂O (1.51% ~ 2.08%) and Na₂O (2.30% ~ 2.62%) with A/NCK (0.77 ~ 0.91), high Al and low Ti with obvious depletion of Nb and Ta. Besides, the Ouxidaban pluton is enriched in large ion lithophile elements (K, Rb, Ba and Pb) and depleted in high field strength elements (Nb, Ta, Zr, Hf, Ti and P), with relatively more light rare earth elements than heavy rare earth elements with the chondrite-normalized rare earth element patterns of slightly right-dipping V-type. These features indicated that Ouxidaban quartz diorite is typical calcium-alkali magmatic rocks which was formed in a subduction stage with a zircon LA-ICP-MS micro area ²⁰⁶Pb/²³⁸U weighted average age of 418.4 ± 2.2Ma. It's widely acknowledged that the north Tarim craton and the south Central-Yili block all have lots of rocks produced by subduction. The ages of the rocks distributed in the southern part of Central-Yili block, ranges from Precambrian to Late Carboniferous and this region does not have an obvious silent time of magma activity. However, the rocks distributed in north Tarim craton whose ages concentrate on 426 ~ 418Ma, except for a granite of 386Ma which is located in east of Ouxidaban pluton and produced by subduction as well. At the same time, there are not a broader magma arc and a peaceful magma activity time in the north Tarim craton. Although a complex tectonic deformation existed there, it wasn't caused by the southward subduction of South Tianshan Ocean. In conclusion, this paper proposes that northern Tarim plate has been transformed from the passive continental margin to active continental margin in Silurian at latest and then it returned to the passive continental margin in Devonian. The evolution of the South Tianshan Ocean during Early Paleozoic was dominated by bidirectional subduction but the southward subduction was short, intermittent or pulse type subduction process until the end of middle Devonian, and the north subduction was a long-term and multi-stage process until the beginning of collision between Central-Yili block and Tarim plate. It should also be noted that the southward subduction process of South Tianshan Ocean was mostly like a normal high-angle subduction.

Key words Ouxidaban quartz diorite; Bidirectional Subduction; South Tianshan Ocean; Northern Tarim craton

摘要 南天山洋的演化历史是中亚造山带研究中关键的问题, 目前对古生代期间南天山洋的俯冲极性、俯冲方式等问题仍然存在着争议。南天山造山带南部地区近东西向出露一系列中酸性侵入岩, 本文以其中的欧西达坂石英闪长岩为对象, 开

* 本文受地质矿产调查评价项目(12120113015600、1212011120293)和国土资源公益性行业专项经费(201211074-05、200911043-13)联合资助。

第一作者简介: 张斌, 男, 1990年生, 硕士生, 地球化学专业, E-mail: zb996897250@163.com

** 通讯作者: 陈文, 男, 1962年生, 研究员, 从事同位素地质年代学研究, E-mail: chenwenf@vip.sina.com

展了系统的岩石学、地球化学和同位素年代学研究。地球化学特征显示其富集 Rb、Ba、K、Pb 等大离子亲石元素,亏损 Nb、Ta、Zr、Hf 等高场强元素,轻稀土元素较重稀土元素富集,稀土配分曲线呈右倾的“海鸥”型,为典型的俯冲成因钙碱性系列岩浆岩,锆石 LA-ICP-MS 微区定年获得 418.4 ± 2.2 Ma 的 $^{206}\text{Pb}/^{238}\text{U}$ 加权平均年龄。结合区域地质背景及前人成果,初步认为塔里木板块北缘至少在志留纪时期已由被动大陆边缘转变成活动大陆边缘,中泥盆世开始又转变为被动大陆边缘;早古生代阶段南天山洋的演化以双向俯冲为主,向南为短期、脉冲式或间歇式的正常高角度俯冲过程,至中泥盆世结束;向北则为长期、多阶段性的俯冲。

关键词 欧西达坂石英闪长岩;双向俯冲;南天山洋;塔里木北缘

中图法分类号 P588.122; P597.3

南天山造山带位于中亚造山带的关键部位,其地质组成与演化一直受到地质学家的广泛关注 (Coleman, 1989; Jahn *et al.*, 2000; 朱志新等, 2008; 郭瑞清等, 2013; Xiao *et al.*, 2013)。南天山碰撞造山带记录着丰富的地质演化信息,带内广泛分布的钨、锡、钼、铜等多金属矿床均与其演化过程密切相关,同时,南天山俯冲消减的过程对于塔里木盆地北部油气藏的形成与保存亦具有重大意义 (李锦轶等, 1992; 毛景文等, 2002; 李曰俊等, 2009; 左国朝和李绍雄, 2011)。但目前对这些成矿作用的地质背景仍存在不同的看法,长期以来,基于构造分析的研究方法,一些学者认为南天山洋在古生代期间一直都是向北俯冲并最终闭合,塔里木北缘一直为被动大陆边缘,而洋盆北缘的伊犁-中天山地块南缘在古生代期间则为活动大陆边缘 (肖序常和汤耀庆, 1991; 刘本培等, 1996; 高俊等, 2006; Xiao *et al.*, 2010; Gao *et al.*, 2011)。而另一些学者对南天山地区的冲断岩片和侵入岩的岩石地球化学研究显示,塔里木北缘在古生代期间已由被动陆缘转化为主动陆缘,并形成了一系列东西向分布的花岗质侵入岩,南天山古洋盆存在南北双向同时俯冲的阶段 (姜常义等, 2001; 夏林圻等, 2007; 朱志新等, 2008; 王超等, 2009; Charvet *et al.*, 2011; Wang *et al.*, 2011; Ge *et al.*, 2012; 郭瑞清等, 2013; Lin *et al.*, 2013; Jiang *et al.*, 2014)。但对南天山洋向南俯冲的方式、俯冲作用的规模及持续的时间等问题尚未进行深入研究。另外,由于南天山古生代形成的地质地貌、构造特征等要素很有可能已经被中生代天山地区强烈的地质活动改造,蛇绿岩产出位置可能与俯冲带位置有一定的差异。因此,本文以南天山碰撞造山带南部 (本文称为塔里木北缘) 地区欧西达坂及色日克亚依拉克一带侵入岩为研究对象,进行了系统的岩石学、地球化学及同位素年代学研究,并结合前人的研究成果,进一步探讨南天山洋在古生代期间的俯冲作用过程,对南天山洋在古生代期间的构造演化提出了新的看法,对南天山地区成矿地质背景的研究具有重要的意义。

1 区域地质背景

南天山造山带位于塔里木地块与伊犁-中天山地块之间,主体为一宽大的碰撞-增生-蛇绿混杂带,其形成与南天山洋的俯冲消减过程、塔里木地块与中天山地块沿中-南天山

缝合线进行的碰撞造山过程密切相关。地质上主要包括南天山洋俯冲消减过程中形成的弧前增生楔以及陆陆碰撞造山过程中形成的构造混杂岩,它代表了碰撞造山发生以前的塔里木地块北缘地区,前寒武纪塔里木基底岩石和附着其上的洋壳增生物质以及部分塔里木地块北缘的陆缘/浅海沉积物均为其组成部分 (李曰俊等, 2001, 2002, 2009; Qian *et al.*, 2009; Gao *et al.*, 2009; 朱志新等, 2009; Han *et al.*, 2011; 黄河, 2013)。南天山造山带以北为那拉提南缘断裂、乌瓦门-拱拜子断裂和卡瓦布拉克断裂,以南为托什干河断裂、塔里木盆地北缘断裂和兴地塔格断裂,在我国境内总体呈向北突出的弧形展布 (图 1a)。不同时期、不同成因类型的花岗岩在南天山均有分布,且以古生代花岗岩类为主 (王超等, 2009; 郭瑞清等, 2013), 志留纪侵入岩主要为偏碱性的花岗岩; 泥盆纪侵入岩主要属于 I 型花岗岩, 形成环境具有从早到晚由消减的活动板块边缘向碰撞带演化的趋势; 石炭纪侵入岩主要为过铝和次铝的钙碱性花岗岩及少量碱性花岗岩, 形成环境为同碰撞和后造山 (朱志新等, 2009)。研究区位于塔里木板块北缘的欧西达坂-色日克亚依拉克一带, 大地构造位置上属于南天山造山带与塔里木盆地交界的盆地过渡区域, 表现为一系列褶皱冲断组合的构造样式 (李向东等, 2004)。样品采集地欧西达坂岩体主体呈近东西处于南天山南缘断裂带中 (图 1b), 主要由石英闪长岩和二长花岗岩组成, 见有韧性变形现象, 中二叠统皮尔包古兹组直接覆盖于该岩体之上。岩体北部地层以泥盆纪萨阿尔明组灰岩、砂岩及板岩为主, 以南为库车前陆盆地, 主要为三叠纪-侏罗纪砂岩、泥岩沉积。色日克亚依拉克地区位于欧西达坂以东, 主要由前寒武系片岩及泥盆纪闪长岩、花岗闪长岩、二长花岗岩构成, 岩体上部为石炭纪残余海盆覆盖, 并分布有碰撞环境下形成的酸性侵入岩及拉张环境下形成的陆相火山岩。

2 岩相学特征

欧西达坂石英闪长岩呈灰黑色, 他形-半自形结构, 块状构造。主要由斜长石、石英、角闪石和少量副矿物组成 (图 2)。斜长石呈他形-半自形板状, 中等绢云母化, 复合双晶特征明显, 后期裂隙垂直于双晶纹发育, 内充填有细粒绢云母; 石英颗粒细小, 形态不规则, 充填于长石颗粒空隙中, 波状消

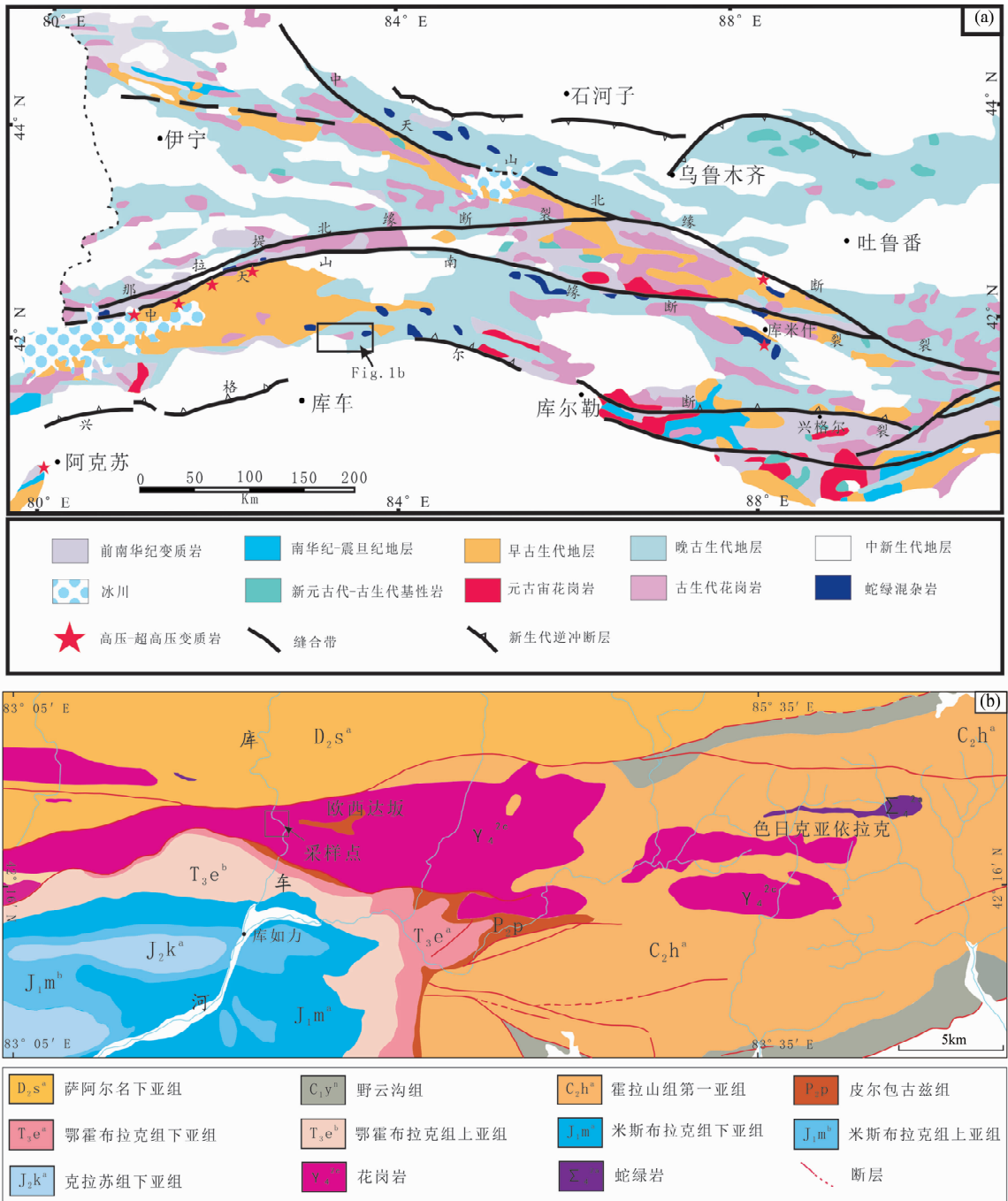


图1 天山地质概况图(a,据高俊等, 2009; Ge *et al.*, 2012; Xu *et al.*, 2012 修改)和欧西达坂地区地质图(b,据新疆地质局区域地质测量大队,1975^①修改)

Fig.1 Simplified geological map of Tianshan Orogen (a, modified after Gao *et al.*, 2009; Ge *et al.*, 2012; Xu *et al.*, 2012) and geological map of Oxidaban region (b)

光,有异常干涉色,经历过变形作用;角闪石多色性明显,绿泥石化、绿帘石化强烈;副矿物主要由锆石、磷灰石等组成。

朱志新等(2008)对色日克亚依拉克一带花岗闪长岩进行了详细的研究,具体的岩相学特征如下:岩石表面呈褐红

色,他形-半自形粒状结构,块状构造。主要由斜长石、钾长石、石英、蚀变暗色矿物和少量副矿物组成。斜长石呈半自形板状、宽板状,有强高岭土化,轻-中度绢云母化,双晶较细密但不清晰;钾长石呈他形粒状,多分布于斜长石四周;石英

① 新疆地质局区域地质测量大队. 1975. 1/20万库勒幅地质图

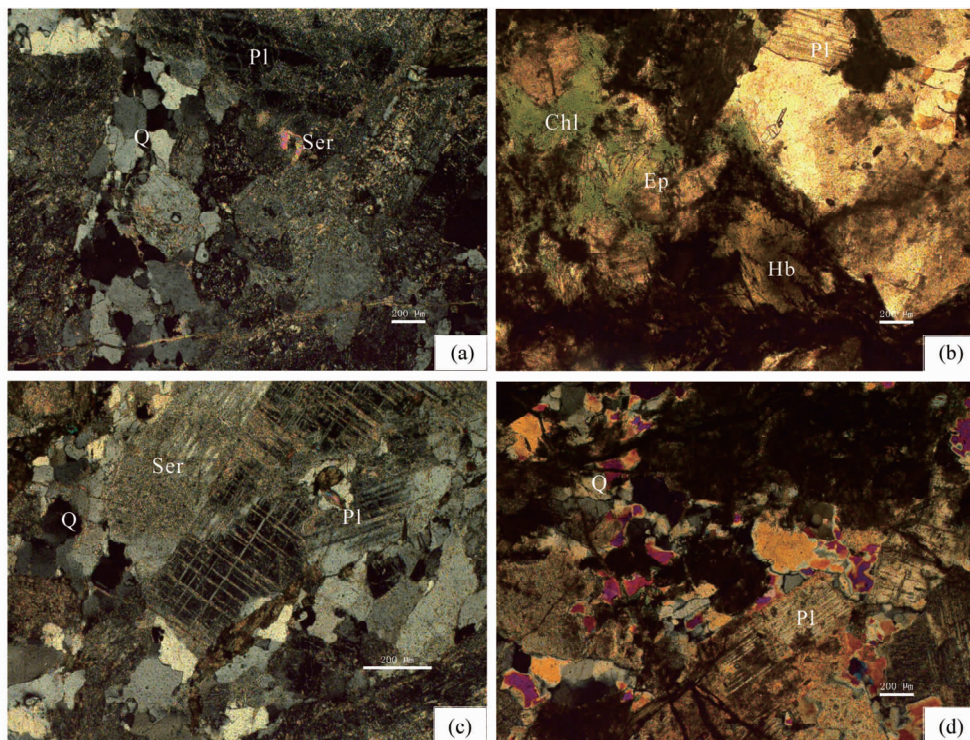


图2 石英闪长岩显微照片

Fig.2 Microscopic photos of Ouxidaban quartz diorite

呈他形粒状,不规则状分布于斜长石孔隙中,具波状消光现象,粒度大小极不等,分布较均匀;蚀变暗色矿物已完全由绿泥石替代,有轻微变形;副矿物少量,由磁铁矿、锆石、磷灰石等组成。

3 岩石地球化学特征及岩石成因研究

欧西达坂样品全岩的主量和微量元素分析均在中国科学院广州地球化学所完成,主量元素分析所用仪器为日本理学 Rigaku100e 型 X 荧光光谱仪,分析误差小于 2%;微量元素分析所用仪器为 Perkin-Elmer Sciex ELAN 6000 ICP-MS,分析误差小于 5%,详细分析流程见刘颖等(1996)和涂湘林等(2011),分析测试结果见表 1。

所测样品石英闪长岩中 SiO_2 含量在 54.23% ~ 56.27%,碱含量($\text{K}_2\text{O} + \text{Na}_2\text{O} = 3.82\% \sim 4.63\%$)低,属于钙碱性系列花岗岩,铝饱和指数 $A/NCK = 0.767 \sim 0.908$,总体为准铝质系列;色日克亚依拉克侵入岩样品亦均为钙碱性系列岩石, $A/NCK = 0.72 \sim 1.05$,另有一二长花岗岩样品 $A/NCK = 1.5$ (朱志新等,2008),总体呈准铝质-过铝质系列。两处岩体均显示出 I 型花岗岩的特征,铝饱和指数为 1.5 的二长花岗岩碱含量较高,且无堇青石出现,推测其为演化程度较高或经过了沉积岩混染的 I 型花岗岩(Chappell, 1999; 王超等, 2009)。下陆壳或上地幔存在高温热源的情况下经脱水熔融通常能产生大量闪长岩,闪长质岩浆中 Al_2O_3 的含

量可作为压力的指示计(Rushmer, 1991; Wolf and Wyllie, 1994; Rapp and Watson, 1995),欧西达坂石英闪长岩 Al_2O_3 含量均大于 15%,因此可将欧西达坂石英闪长岩的成岩压力限定在 1600 ~ 1800MPa 之间,色日克亚依拉克侵入岩中闪长岩 Al_2O_3 含量均低于 15%,其成岩压力可限定在 1600MPa 以下,两处岩体的成岩条件不同表明岩浆侵位深度不一致。

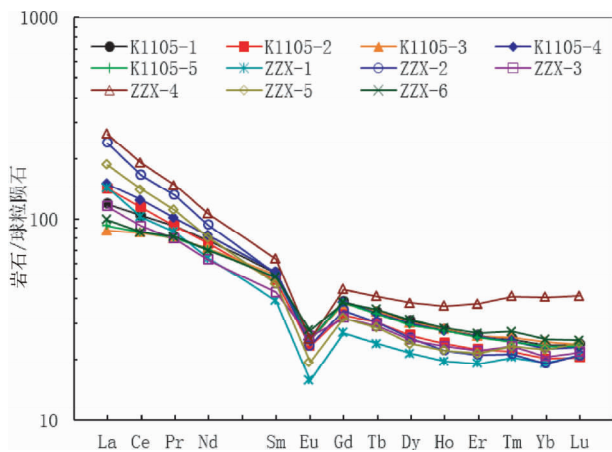


图3 稀土元素球粒陨石标准化分布型式图(标准化值据 Sun and McDonough, 1989)

色日克亚依拉克岩体数据引自朱志新等(2008)

Fig. 3 The chondrite-normalized rare earth elements (normalization values after Sun and McDonough, 1989)

The data of Serikeyayilake from Zhu *et al.* (2008)

表1 欧西达坂石英闪长岩主量(wt%)、微量($\times 10^{-6}$)元素分析结果Table 1 Major (wt%) and trace ($\times 10^{-6}$) elements analyses of Ouxidaban quartz diorite

样品号	K1105-1	K1105-2	K1105-3	K1105-4	K1105-5
SiO ₂	55.68	56.27	54.23	55.69	55.01
TiO ₂	1.07	0.92	0.98	1.08	0.99
Al ₂ O ₃	15.27	16.03	15.49	15.15	15.19
Fe ₂ O ₃	9.63	8.29	9.33	9.62	9.44
CaO	6.65	6.44	7.56	6.59	7.14
MgO	5.10	4.38	4.81	5.11	4.97
K ₂ O	1.53	1.51	2.08	1.61	1.73
Na ₂ O	2.30	2.62	2.55	2.32	2.43
MnO	0.14	0.12	0.14	0.14	0.14
P ₂ O ₅	0.20	0.18	0.20	0.20	0.21
LOI	1.94	2.76	2.13	1.98	2.28
Total	99.51	99.52	99.51	99.50	99.54
Sc	37.75	33.5	34.69	36.6	33.89
Ti	6453	6029	5705	6642	6025
V	252.9	241.4	236.8	254.1	234.9
Cr	69.55	69.35	71.76	69.65	68.49
Mn	1087	992.5	1073	1091	1116
Co	29.3	26.17	27.56	30.03	28.45
Ni	32.62	30.15	30.98	34.6	31.76
Cu	55.72	59.1	51.47	63.02	37.78
Zn	85.46	74.81	77.33	85.35	79.74
Ga	18.71	18.58	18.53	18.42	18.47
Ge	1.828	1.77	1.932	1.771	1.958
Rb	51.5	49.3	73.7	55.8	61.4
Sr	280	330	276	274	276
Zr	197	139	170	156	127
Nb	9.385	8.256	9.097	9.808	9.473
Cs	2.032	1.488	0.941	1.733	0.939
Ba	325	352	432	339	357
La	28.11	33.64	20.75	35.51	21.88
Ce	63.49	69.91	52.17	75.96	52.43
Pr	8.745	8.807	7.593	9.603	7.651
Nd	36.48	35.13	33.26	38.63	32.72
Sm	8.243	7.519	8.084	8.325	7.826
Eu	1.462	1.345	1.436	1.445	1.461
Gd	7.942	6.844	7.736	7.896	7.849
Tb	1.287	1.131	1.287	1.266	1.257
Dy	7.896	6.646	7.705	7.662	7.507
Ho	1.588	1.356	1.596	1.569	1.562
Er	4.329	3.689	4.298	4.295	4.221
Tm	0.641	0.558	0.655	0.63	0.622
Yb	3.972	3.418	4.134	3.832	3.948
Lu	0.601	0.517	0.599	0.581	0.589
Y	38.32	32.95	39.15	38.76	38.48
Hf	5.423	3.769	4.614	4.154	3.552
Ta	0.734	0.595	0.664	0.706	0.701
Pb	9.887	10.17	7.381	9.258	7.316
Th	9.578	11.72	4.937	13.62	5.613
U	1.376	1.078	1.502	1.249	1.270

欧西达坂与色日克亚依拉克岩体都具有相似的稀土配分型式(图3),整体呈右倾海鸥式分布曲线。欧西达坂石英闪长岩稀土总量 ΣREE 为 $151.3 \times 10^{-6} \sim 197.2 \times 10^{-6}$, $LREE/HREE = 4.40 \sim 6.47$, $(La/Yb)_N = 3.60 \sim 7.06$,轻重稀土分馏特征明显,轻稀土元素相对重稀土元素更富集, $\delta Eu = 0.54 \sim 0.56$,具有明显的Eu负异常,表明在岩浆源区具有斜长石的残留或经历了较强的斜长石的分离结晶;色日克亚依拉克侵入岩稀土总量 ΣREE 为 $152.2 \times 10^{-6} \sim 292.1 \times 10^{-6}$, $LREE/HREE = 4.36 \sim 9.40$, $(La/Yb)_N = 3.98 \sim 12.59$,轻重稀土分馏较欧西达坂石英闪长岩更为明显,部分样品具有更加突出的Eu负异常, $\delta Eu = 0.48 \sim 0.69$ 。平坦的重稀土配分型式及较低的Sr/Y比值指示了形成岩体的弧岩浆的亲缘性。

从微量元素原始地幔标准化配分模式图(图4)中可看出Rb、Ba、K、Pb等大离子亲石元素明显富集,Th、Nb、Ta、P、Zr、Hf、Ti等高场强元素亏损,具有正常弧花岗岩的特征,Nb、Ta的亏损表明岩浆来源于与俯冲作用相关的地壳部分熔融或壳幔混合(Dungan *et al.*, 1986; Foley, 1992)。高Al低Ti及明显的Nb、Ti、P异常说明样品形成于大陆板块边缘或岛弧环境。欧西达坂石英闪长岩K/Rb比值在233.2~253.5,均大于200,表明岩浆分异或水热作用不明显(Dostal and Chatterjee, 2000);而色日克亚依拉克侵入岩的情况则有所不同,2个二长花岗岩及1个花岗闪长岩的K/Rb比值在153.2~172.2,说明岩浆在岩体形成过程中经历了较高度度的演化,受水热作用的影响较显著。以上特征反应出欧西达坂岩体与色日克亚依拉克侵入岩在形成环境上的差别。

在微量元素Y-Nb和Y+Nb-Rb构造环境判别图解上(图5),欧西达坂岩体与色日克亚依拉克侵入岩共计11个岩石样品中有10个投入火山弧区,其构造背景总体显示与

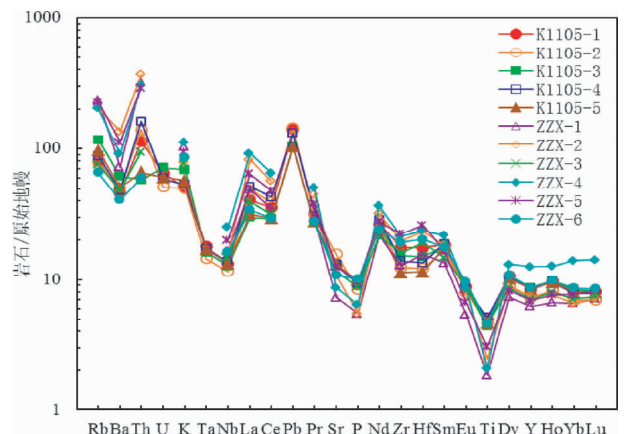


图4 微量元素原始地幔标准化蛛网图(标准化值据Sun and McDonough, 1989)

色日克亚依拉克岩体数据引自朱志新等(2008)

Fig. 4 The primitive mantle-normalized multi-element plots (normalization values after Sun and McDonough, 1989)

The data of Serikeyayilake from Zhu *et al.* (2008)

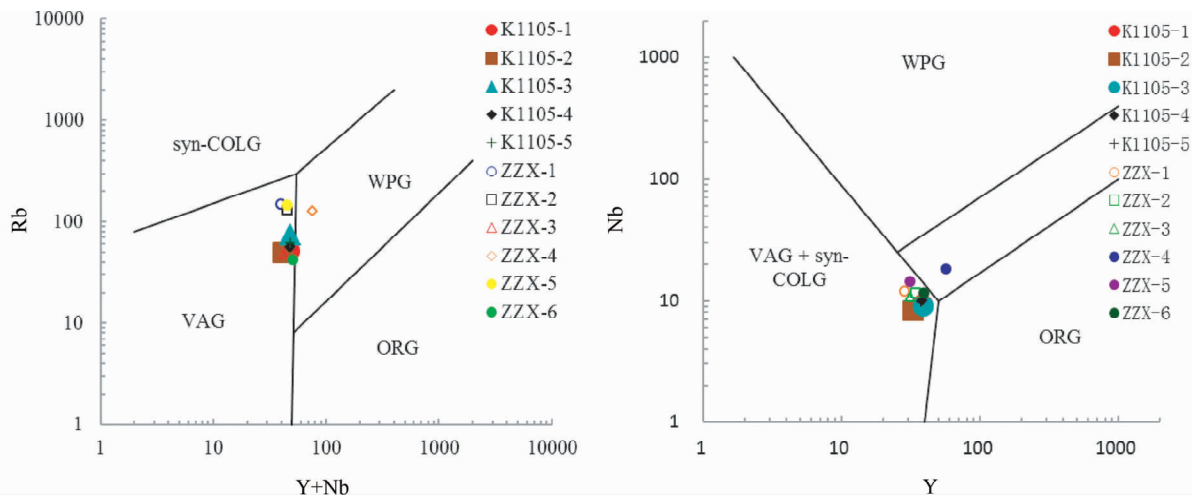


图5 微量元素构造环境判别图解

WPG-板内花岗岩; VAG-火山弧花岗岩; ORG-洋中脊花岗岩; Syn-COLG-同造山花岗岩

Fig. 5 Tectonic environment discrimination of trace elements

WPG-intraplate granites; VAG-volcanic arc granites; ORG-ocean ridge granites; Syn-COLG-syn-collisional granite

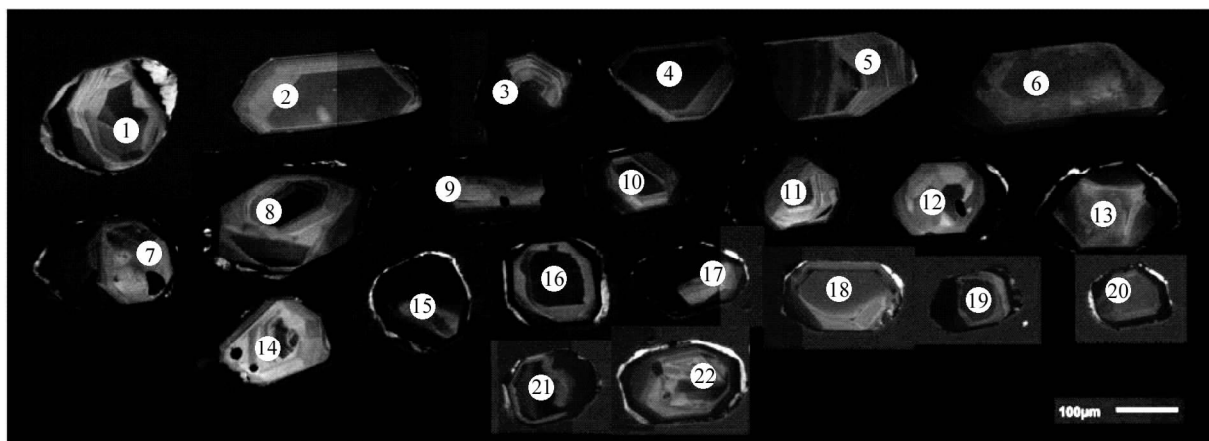


图6 欧西达坂石英闪长岩锆石阴极发光图像

Fig. 6 CL images of zircons for Ouxidaban quartz diorite

板块构造活动形成的火山弧花岗岩有关,可能为活动陆缘的产物。

结合上述地球化学特征,说明欧西达坂岩体与色日克亚依拉克岩体大体上具有相同的岩石成因,其形成均与板块活动相关,形成于活动大陆边缘,但岩体侵位深度、形成时的温度压力条件等具体环境仍存在一定差别。王超等(2009)对欧西达坂花岗岩的岩石成因进行了更加深入细致的研究,结论与本文一致,因此本文未对岩石成因方面的问题进行详细探讨。

4 同位素年代学研究

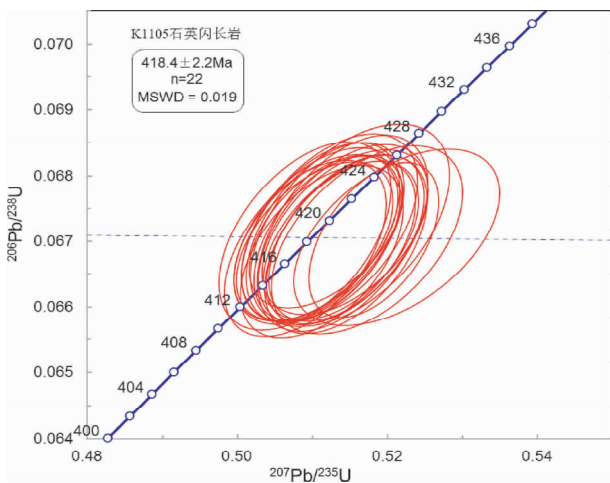
为确定构造热事件发生的时间,本文从欧西达坂石英闪长岩中选取锆石进行 LA-ICP-MS 定年。新鲜的全岩样品通

过人工重砂法分选出锆石后在双目显微镜下挑选出透明、无裂隙、无包裹体的自形锆石颗粒,在玻璃板上用环氧树脂固定,待环氧树脂充分固化后抛光至锆石露出核部,然后进行锆石的阴极发光显微成像。锆石的制靶及 CL 图像分析均在北京锆年领航科技有限公司完成;LA-ICP-MS 锆石 U-Pb 定年测试在香港大学地球科学系完成,所用仪器为 VG PQ Excell ICP-MS 及与之配套的 New Wave UP213 激光剥蚀系统,激光剥蚀所用束斑直径 30µm,频率 6Hz,剥蚀时间 30 ~ 60s,剥蚀深度 20 ~ 40µm。为保证测试的精确度及准确度,对每个锆石颗粒进行测试前均在样品表面先进行 10s 的剥蚀以排除普通铅的污染。锆石年龄采用国际标准锆石 91500 进行外标校正,分析过程中每隔 5 个样品分析点进行一个标样校正,以保证标样和样品的仪器条件完全一致(Xia *et al.*, 2004)。

表 2 欧西达坂石英闪长岩中锆石的 LA-ICP-MS U-Pb 同位素分析结果

Table 2 LA-ICP-MS U-Pb data for zircons from Ouxidaban quartz diorite

测点号	Th/U	同位素比值						同位素年龄值 (Ma)							
		$\frac{^{207}\text{Pb}}{^{206}\text{Pb}}$	1σ	$\frac{^{207}\text{Pb}}{^{235}\text{U}}$	1σ	$\frac{^{206}\text{Pb}}{^{238}\text{U}}$	1σ	$\frac{^{238}\text{U}}{^{232}\text{Th}}$	1σ	$\frac{^{207}\text{Pb}}{^{206}\text{Pb}}$	1σ	$\frac{^{207}\text{Pb}}{^{235}\text{U}}$	1σ	$\frac{^{206}\text{Pb}}{^{238}\text{U}}$	1σ
K1105-1	0.63	0.05527	0.00019	0.51181	0.00677	0.06715	0.00077	1.66	0.02	423	13	420	5	419	5
K1105-2	0.72	0.05549	0.00021	0.51123	0.00716	0.06684	0.00087	1.51	0.02	432	14	419	5	417	5
K1105-3	0.57	0.05566	0.00017	0.51451	0.00684	0.06705	0.00084	1.81	0.02	439	13	421	5	418	5
K1105-4	0.89	0.05553	0.00021	0.51498	0.00876	0.06724	0.00102	1.37	0.01	433	17	422	6	420	6
K1105-5	0.74	0.05567	0.00021	0.51379	0.00656	0.06698	0.00082	1.45	0.01	439	13	421	4	418	5
K1105-6	0.69	0.05564	0.00024	0.51378	0.00683	0.06701	0.0008	1.56	0.02	438	13	421	5	418	5
K1105-7	0.89	0.05554	0.00021	0.51434	0.00731	0.06714	0.00083	1.23	0.01	434	14	421	5	419	5
K1105-8	0.81	0.05518	0.00016	0.50903	0.00712	0.06689	0.00089	1.39	0.01	419	14	418	5	417	5
K1105-9	0.47	0.05519	0.00017	0.51074	0.0074	0.06708	0.00089	2.2	0.02	420	14	419	5	419	5
K1105-10	0.83	0.05521	0.00024	0.51043	0.00722	0.06705	0.00084	1.37	0.01	421	14	419	5	418	5
K1105-11	0.57	0.05529	0.00022	0.51226	0.00775	0.0672	0.00095	1.89	0.02	424	15	420	5	419	6
K1105-12	0.79	0.05533	0.00022	0.51167	0.00695	0.06713	0.00091	1.36	0.01	426	14	420	5	419	6
K1105-13	0.95	0.05626	0.00022	0.52121	0.00906	0.06706	0.00089	1.16	0.01	463	18	426	6	418	5
K1105-14	0.88	0.05504	0.00021	0.50899	0.00757	0.06708	0.00095	1.27	0.01	414	15	418	5	419	6
K1105-15	0.76	0.05556	0.00019	0.51407	0.00745	0.0671	0.00091	1.45	0.01	435	14	421	5	419	5
K1105-16	1.01	0.05522	0.00016	0.51107	0.00696	0.06714	0.0009	1.06	0.01	421	14	419	5	419	5
K1105-17	0.73	0.05576	0.00022	0.51443	0.00715	0.06695	0.0009	1.45	0.01	443	14	421	5	418	5
K1105-18	1.01	0.05558	0.00018	0.514	0.00751	0.06712	0.00099	1.07	0.01	435	15	421	5	419	6
K1105-19	0.98	0.05595	0.00021	0.51725	0.00841	0.06702	0.00095	1.11	0.01	450	16	423	6	418	6
K1105-20	0.79	0.05523	0.0002	0.51027	0.00689	0.067	0.0008	1.43	0.01	422	13	419	5	418	5
K1105-21	0.99	0.0554	0.00017	0.51193	0.00643	0.06704	0.00083	1.09	0.01	429	13	420	4	418	5
K1105-22	0.98	0.05614	0.0002	0.51816	0.00571	0.06702	0.00078	1.12	0.01	458	12	424	4	418	5

图 7 欧西达坂石英闪长岩锆石 $^{206}\text{Pb}/^{238}\text{U}$ - $^{207}\text{Pb}/^{235}\text{U}$ 年龄谐和图Fig. 7 Zircon $^{206}\text{Pb}/^{238}\text{U}$ - $^{207}\text{Pb}/^{235}\text{U}$ concordia diagram of the Ouxidaban quartz diorite

锆石 U-Pb 定年分析结果见表 2, 所选锆石大部分呈短柱状, 少部分长柱状锆石长宽比约为 2:1, 晶形完整。阴极发光图像(图 6) 显示锆石具有明显的环带构造, 颗粒核部和边部清晰, Th/U 比值在 0.47~1.01 之间, 平均为 0.80, 这些特征均显示所测锆石为典型的岩浆成因锆石。

欧西达坂石英闪长岩中选出的 22 个锆石颗粒 $^{206}\text{Pb}/^{238}\text{U}$ 年龄集中分布在 417~420Ma 之间, 分析结果均落在谐和曲线上或其附近, $^{206}\text{Pb}/^{238}\text{U}$ 加权平均年龄为 $418.4 \pm 2.2\text{Ma}$, $\text{MSWD} = 0.019$ (图 7), 数据处理方式见 Ludwig (2001) 及 Liu *et al.* (2010)。分析结果显示外误差小于内误差, 这种情况与仪器的测试能力不足及系统精度不够有关, 但与王超等 (2009) 在同一地点获得的 $421 \pm 3\text{Ma}$ 的锆石 U-Pb 年龄在误差范围内一致, 表明仪器系统精度对本文所获得的年龄的准确性影响并不大, 测试结果仍然是可信的。结合锆石 CL 图像特征及锆石 Th/U 比值, 此年龄代表了岩浆锆石的冷却年龄, 也最接近于岩石的形成年龄。

欧西达坂以东色日克亚依拉克一带花岗闪长岩中岩浆锆石 SHRIMP 年龄为 $382.1 \pm 6.2\text{Ma}$ ($\text{MSWD} = 1.8$), 代表了稍晚一期岩浆活动的时间, 另有一组捕获锆石年龄为 $419.0 \pm 6.5\text{Ma}$ ($\text{MSWD} = 1.14$) (朱志新等, 2008), 与欧西达坂石英闪长岩形成时间在误差范围内一致, 这反应了中志留世期间塔里木北缘地区发生的一次岩浆热事件。

5 讨论

5.1 南天山洋俯冲的岩石学证据

塔里木北缘断续出露的侵入岩带西起老虎台, 经黑英山、密勒洞、野云沟至库尔勒一带(郭瑞清等, 2013), 其岩石

组合主要为橄榄辉长岩-辉长岩-辉长闪长岩-闪长岩-石英闪长岩-花岗岩(姜常义等,2001)。其中库尔干南岩体主要由石英闪长岩及黑云斜长花岗岩组成(徐学义等,2006;夏林圻等,2007);色日克亚依拉克侵入岩则包括闪长岩、二长花岗岩及花岗闪长岩(朱志新等,2008);欧西达坂岩体主要由石英闪长岩、二长花岗岩组成(王超等,2009);库尔勒一带博斯腾乡岩体的主体为黑云石英闪长岩,铁门关岩体岩性为似斑状花岗闪长岩(郭瑞清等,2013);铁热克岩体主体为二长岩(黄河,2013)。这些岩石组合均为钙碱性系列岩石,均具有高场强元素亏损,大离子亲石元素富集的地球化学特征,且均形成于早古生代时期(姜常义等,2001;夏林圻等,2007;朱志新等,2008;王超等,2009;郭瑞清等,2013;黄河,2013),具有大陆弧花岗岩的特点,与安第斯型活动大陆边缘火成岩的岩石学和地球化学特征有很大的相似性(Briqueu *et al.*, 1984; Pearce and Peate, 1995; Högdahl *et al.*, 2008; Ge *et al.*, 2012),这一系列近东西向分布的中酸性岩石表明塔里木北缘至少在早古生代末志留纪时期已由被动大陆边缘转化为活动大陆边缘,这些岩体的形成均与洋壳俯冲作用有关,南天山洋在早古生代时期存在向南俯冲至塔里木板块之下的过程。

中天山-伊犁板块南缘沿尼古拉耶夫线广泛出露的大哈拉军山组火山岩以粗面安山岩、粗面岩、流纹岩、中酸性凝灰岩为主,均具有典型大陆弧岩浆的地球化学特征,代表了南天山洋的火山岛弧环境(朱永峰等,2005);巴仑台以北地区出露的糜棱岩化中-酸性侵入岩元素地球化学特征显示其属于火山弧环境(杨天南等,2006);西天山伊犁地块南缘出露的大量古生代侵入岩其岩石学和地球化学特征均显示出典型活动陆缘侵入岩的特征(朱志新等,2006; Long *et al.*, 2011);巴音布鲁克镇以北石英辉长岩、库米什北-托克逊南志留纪-早泥盆世碱长花岗岩及黑云母花岗岩、库尔干南斜长花岗岩等配分型式均与火山弧花岗岩类似(徐学义等,2006);比开地区广泛出露的花岗岩和花岗闪长岩均具有钙碱性大陆弧花岗岩特征(龙灵利等,2007);库米什地区黄尖山岩体的地球化学特征指示其为活动大陆边缘俯冲带岛弧演化的产物(张成立等,2007)。这些广布于中天山南缘的岛弧岩浆岩很好的证实了南天山洋盆向伊犁-中天山板块之下的北向俯冲作用。

5.2 南天山洋俯冲阶段的时代约束

目前塔里木北缘地区出露的俯冲成因的岩体形成时间集中在 426.3 ~ 404.8Ma(徐学义等,2006;王超等,2009; Ge *et al.*, 2012; 郭瑞清等,2013;黄河,2013; Lin *et al.*, 2013),另有色日克亚依拉克岩体形成于 386Ma(朱志新等,2008)及柳树沟以东钾长花岗岩形成于 388.1 ± 2.2Ma(Lin *et al.*, 2013),已公开发表的资料中未见塔里木北缘地区其它时期俯冲成因岩体的出露,且中泥盆世至中石炭世之间的岩浆活动记录缺乏,砂岩中也少见此时期的碎屑锆石,砂岩中

碎屑锆石记录的岩浆活动时间主要集中于 462 ~ 395Ma 和 302 ~ 276Ma 两个年龄区间(Ge *et al.*, 2012; 黄河,2013),此外,塔里木北缘地区广泛存在的被动陆缘环境下形成的下泥盆统至石炭系浅海相地层,说明在此岩浆活动间歇期塔里木地块北缘又重新转变成被动大陆边缘(Han *et al.*, 2011; 黄河,2013)。以上证据说明南天山洋向南俯冲持续的时间并不长,至中泥盆世向南俯冲的过程已结束。且欧西达坂岩体与色日克亚依拉克岩体虽具有相同的岩石成因,但除了具有不同的形成时间外,根据其地球化学特征的差异,两处岩体形成时的侵位深度、受流体的影响程度及成岩的温度压力条件等均存在较大的差别,表明二者是在南天山洋俯冲作用的不同阶段形成的。综上,南天山洋向南的俯冲作用可能为短期的至少两阶段的脉冲式或间歇式过程,此外塔里木北缘俯冲成因岩体出露规模都不大,表明南天山洋向南的俯冲作用并不强烈,仅为南天山洋多期收缩和陆缘增生演化过程中的一个小插曲(图8)。

与塔里木北缘地区相对应,中天山南缘地区岩浆活动持续长,并未见长时间明显的构造-岩浆活动间歇期,在 490 ~ 310Ma 未见明显的年龄间断,主要发育于 490 ~ 436Ma、419 ~ 393Ma、370 ~ 366Ma 及 354 ~ 313Ma 四个年龄段,中天山南缘的高压-超高压变质时代也具有多期性,主要集中在 415 ~ 390Ma 和 370 ~ 345Ma 两个年龄段(王润三等,1998;高俊等,2000;周鼎武等,2004;朱永峰等,2005;杨天南等,2006;高俊等,2006;朱志新等,2006;徐学义等,2006;龙灵利等,2007;张成立等,2007;王超等,2009; Long *et al.*, 2011; Gao *et al.*, 2011; Jiang *et al.*, 2014),显示了多期构造-岩浆活动的特征,表明伊犁-中天山地块在中泥盆世-中石炭世之间岩浆活动依然频繁,南天山洋向伊犁-中天山地块

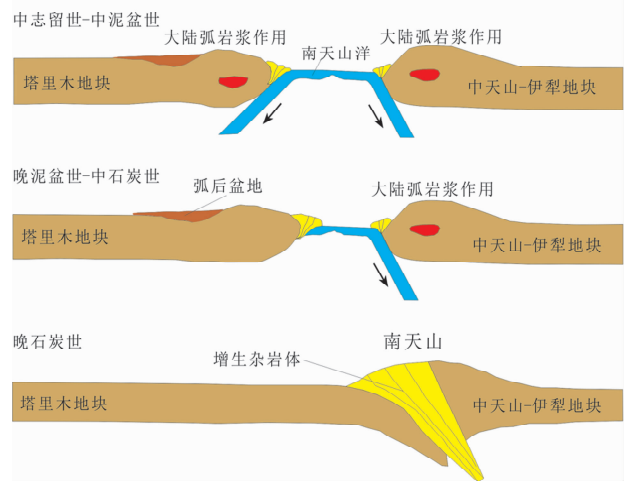


图8 南天山洋古生代期间俯冲模型(据 Ge *et al.*, 2012 修改)

Fig. 8 The subduction model of South Tianshan Ocean during the Paleozoic (modified after Ge *et al.*, 2012)

之下的俯冲作用具有长期、多阶段的特点(图8)。

5.3 南天山洋俯冲方式

王超等(2009)认为南天山古洋盆向南俯冲的过程为低角度板片俯冲。低角度平坦俯冲一般具有异常宽阔的岩浆弧带及较长的弧岩浆静寂期,且上覆板块表现为较复杂的变形构造。塔里木北缘地区近东西向虽出露一些钙碱性岩浆岩,但分布范围窄,出露面积小,明显不能构成一条宽阔的岩浆弧带,同时,中泥盆世-中石炭世期间塔里木北缘地区虽无岩浆活动的记录,形成了弧岩浆的静寂期,但中石炭世之后该地区的岩浆活动多为碰撞造山诱发的而与板块的俯冲作用无关,古南天山洋向南的俯冲作用在中泥盆世已经结束,因此南天山洋向南俯冲过程中所谓的弧岩浆静寂期也是不存在的。南天山造山带南部前陆褶皱冲断带主要形成发育时限为晚泥盆世-早石炭世(李向东等,1998,2004;李向东和王克卓,2000),此时南天山古洋盆向南的俯冲作用已结束,但向北俯冲到伊犁-中天山地块之下的作用却仍在进行,考虑到此构造变形带的规模、构造样式及发育时限(张传恒等,1998;Chen *et al.*, 1999;李向东和王克卓,2000;李向东等,2004;王清华,2007),将其解释为南天山洋向北俯冲至伊犁-中天山地块之下的产物更加合理。以上研究结果及南天山地质演化特征表明南天山洋向南平坦俯冲的特征并不明显,更可能为正常俯冲形式。

6 结论

(1)南天山洋早古生代期间同时存在向南北两侧双向俯冲的情况,塔里木板块北缘至少在志留纪时期已由被动大陆缘转变成活动大陆边缘,中泥盆世开始又转变为被动大陆边缘。

(2)南天山洋向南为短期、脉冲式或间歇式的俯冲作用,至中泥盆世结束;向北则为长期、多阶段性的俯冲作用。早古生代期间南天山洋的演化以双向俯冲为主,中泥盆世-中石炭世向南俯冲结束,南天山洋的演化主要为向北的俯冲作用。

(3)南天山洋向南的俯冲作用更可能为正常的高角度俯冲,低角度板片俯冲的特征并不明显。

致谢 锆石单颗粒的挑选工作在河北省区域地质矿产调查所实验室完成,锆石 U-Pb 定年及数据处理得到香港大学地球科学系耿红燕博士、Wong Jean 博士的帮助;全岩样品的主微量数据测试工作得到中国科学院广州地球化学研究所刘颖高级工程师的指导;在此一并表示衷心的感谢!

References

Briqueu L, Bougault H and Joron JL. 1984. Quantification of Nb, Ta, Ti

- and V anomalies in magmas associated with subduction zones: Petrogenetic implications. *Earth and Planetary Science Letters*, 68 (2): 297–308
- Chappell BW. 1999. Aluminium saturation in I- and S-type granites and the characterization of fractionated haplogranites. *Lithos*, 46 (3): 535–551
- Charvet J, Shu LS, Laurent CS, Wang B, Faure M, Cluzel D, Chen Y and De Jong K. 2011. Palaeozoic tectonic evolution of the Tianshan belt, NW China. *Science China (Earth Sciences)*, 54 (2): 166–184
- Chen CM, Lu HF, Jia D, Cai DS and Wu SM. 1999. Closing history of the southern Tianshan oceanic basin, western China: An oblique collisional orogeny. *Tectonophysics*, 302(1–2): 23–40
- Coleman RG. 1989. Continental growth of Northwest China. *Tectonics*, 8 (3): 621–635
- Dostal J and Chatterjee AK. 2000. Contrasting behaviour of Nb/Ta and Zr/Hf ratios in a peraluminous granitic pluton (Nova Scotia, Canada). *Chemical Geology*, 163(1): 207–218
- Dungan MA, Lindstrom MM, Mcmillan NJ, Moorbath S, Hoefs J and Haskin LA. 1986. Open system magmatic evolution of the Taos Plateau volcanic field, northern New Mexico: 1. The petrology and geochemistry of the Servilleta Basalt. *Journal of Geophysical Research: Solid Earth (1978–2012)*, 91(B6): 5999–6028
- Foley S. 1992. Petrological and characterization of the source components of potassic magmas: Geochemical and experimental constraints. *Lithos*, 28(3): 187–204
- Gao J, Zhang LF and Liu SW. 2000. The $^{40}\text{Ar}/^{39}\text{Ar}$ age record of formation and uplift of the blueschists and eclogites in the western Tianshan Mountains. *Chinese Science Bulletin*, 45(1): 89–94 (in Chinese)
- Gao J, Long LL, Qian Q, Huang DZ, Su W and Klemm R. 2006. South Tianshan: A Late Paleozoic or a Triassic orogen? *Acta Petrologica Sinica*, 22(5): 1049–1061 (in Chinese with English abstract)
- Gao J, Long LL, Klemm R, Qian Q, Liu DY, Xiong XM, Su W, Liu W, Wang YT and Yang FQ. 2009. Tectonic evolution of the South Tianshan orogen and adjacent regions, NW China: Geochemical and age constraints of granitoid rocks. *International Journal of Earth Sciences*, 98(6): 1221–1238
- Gao J, Qian Q, Long LL, Zhang X, Li JL and Su W. 2009. Accretionary orogenic process of western Tianshan, China. *Geological Bulletin of China*, 28(12): 1804–1816 (in Chinese)
- Gao J, Klemm R, Qian Q, Zhang X, Li JL, Jiang T and Yang YQ. 2011. The collision between the Yili and Tarim blocks of the southwestern Altaids: Geochemical and age constraints of a leucogranite dike crosscutting the HP-LT metamorphic belt in the Chinese Tianshan Orogen. *Tectonophysics*, 499(1): 118–131
- Ge RF, Zhu WB, Wu HL, Zheng BH, Zhu XQ and He JW. 2012. The Paleozoic northern margin of the Tarim Craton: Passive or active? *Lithos*, 142: 1–15
- Guo RQ, Nijati A, Qin Q, Jia XL, Zhu ZX, Wang KZ and Li YP. 2013. Geological characteristics and tectonic significance of Silurian granitic intrusions in the northern Tarim craton, Xinjiang. *Geological Bulletin of China*, 32(2–3): 220–238 (in Chinese with English abstract)
- Han BF, He GQ, Wang XC and Guo ZJ. 2011. Late Carboniferous collision between the Tarim and Kazakhstan-Yili terranes in the western segment of the South Tianshan Orogen, Central Asia, and implications for the North Xinjiang, western China. *Earth-Science Reviews*, 109(3): 74–93
- Högdahl K, Sjöström H, Andersson UB and Ahl M. 2008. Continental margin magmatism and migmatization in the west-central Fennoscandian Shield. *Lithos*, 102(3): 435–459
- Huang H. 2013. Paleozoic granitoids in the Chinese South Tianshan and its implications for geological evolution of the region. Ph. D. Dissertation. Beijing: Chinese University of Geosciences, 1–144 (in Chinese with English summary)
- Jahn BM, Wu FY and Chen B. 2000. Granitoids of the Central Asian Orogenic Belt and continental growth in the Phanerozoic.

- Transactions of the Royal Society of Edinburgh: Earth Sciences, 91 (1-2): 181-194
- Jiang CY, Mu YM, Zhao XN, Bai KY and Zhang HB. 2001. Petrology and geochemistry of an active continental-margin intrusive rock belt on the northern margin of the Tarim plate. *Regional Geology of China*, 20(2): 158-163 (in Chinese with English abstract)
- Jiang T, Gao J, Klemm R, Qian Q, Zhang X, Xiong XM, Wang XS, Tan Z and Chen BX. 2014. Paleozoic ophiolitic mélanges from the South Tianshan Orogen, NW China: Geological, geochemical and geochronological implications for the geodynamic setting. *Tectonophysics*, 612-613: 106-127
- Li JY, Xiao XC, Tang YQ, Zhao M, Feng YM and Zhu BQ. 1992. Metal deposits and plate tectonics in Northern Xinjiang. *Xinjiang Geology*, 10(2): 138-146 (in Chinese with English abstract)
- Li XD, Wang QM and Wang KZ. 1998. New information of post-collisional evolution of the Tianshan Mountains: Evidence from dynamic metamorphic rocks from the middle sector of Awulale range. *Geological Review*, 44(4): 443-448 (in Chinese with English abstract)
- Li XD and Wang KZ. 2000. On orogenic to basinal tectonic transfer along the southern margin of West Tianshan Mountains, China. *Xinjiang Geology*, 18(3): 211-219 (in Chinese with English abstract)
- Li XD, Xiao WJ and Zhou ZL. 2004. $^{40}\text{Ar}/^{39}\text{Ar}$ age determination on the Late Devonian tectonic event along the southern margin of the South Tianshan Mountains and its significance. *Acta Petrologica Sinica*, 20(3): 691-696 (in Chinese with English abstract)
- Li YJ, Song WJ, Mai GR, Zhou LX, Hu JF and Shang XL. 2001. Characteristics of Kuqa and northern Tarim foreland basins and their coupling relation to South Tianshan orogen. *Xinjiang Petroleum Geology*, 22(5): 376-381 (in Chinese with English abstract)
- Li YJ, Wang ZM, Mai GR, Wu HR, Huang ZB and Tan ZJ. 2002. New discovery of radiolarian fossils from Aiktik Group in Tarim basin and its significance. *Xinjiang Petroleum Geology*, 23(6): 496-500 (in Chinese with English abstract)
- Li YJ, Yang HJ, Zhao Y, Luo JC, Zheng DM and Liu YL. 2009. Tectonic framework and Evolution of South Tianshan, NW China. *Geotectonica et Metallogenia*, 33(1): 94-104 (in Chinese with English abstract)
- Lin W, Chu Y, Ji WB, Zhang ZP, Shi YH, Wang ZY, Li Z and Wang QC. 2013. Geochronological and geochemical constraints for a Middle Paleozoic continental arc on the northern margin of the Tarim block: Implications for the Paleozoic tectonic evolution of the South Chinese Tianshan. *Lithos*, 5(4): 355-381
- Liu BP, Wang ZQ and Zhang CH. 1996. *The Tectonic Framework and Evolution in Southwest Tianshan Mountains, China*. Wuhan: Press of China University of Geosciences, 1-120 (in Chinese)
- Liu Y, Liu HC and Li XH. 1996. Simultaneous and precise determination of 40 trace elements in rock samples using ICP-MS. *Geochimica*, 25(6): 552-558 (in Chinese with English abstract)
- Liu YS, Gao S, Hu ZC, Gao CG, Zong KQ and Wang DB. 2010. Continental and oceanic crust recycling-induced melt-peridotite interactions in the Trans-North China Orogen: U-Pb dating, Hf isotopes and trace elements in zircons from mantle xenoliths. *Journal of Petrology*, 51(1-2): 537-571
- Long LL, Gao J, Xiong XM and Qian Q. 2007. Geochemistry and geochronology of granitoids in Bikai region, southern Central-Tianshan mountains, Xinjiang. *Acta Petrologica Sinica*, 23(4): 719-732 (in Chinese with English abstract)
- Long LL, Gao J, Klemm R, Beier C, Qian Q, Zhang X, Wang J and Jiang T. 2011. Geochemical and geochronological studies of granitoid rocks from the Western Tianshan Orogen: Implications for continental growth in the southwestern Central Asian Orogenic Belt. *Lithos*, 126(3): 321-340
- Ludwig KR. 2001. *Isoplot/Ex, Rev. 2.49: A Geochronological Toolkit for Microsoft Excel*. Berkeley Geochronological Center, Special Publication, (1a): 55
- Mao JW, Han CM, Wang YT, Yang JM and Wang ZL. 2002. Geological characteristics, metallogenic model and criteria for exploration of the large South Tianshan gold metallogenic belt in Central Asia. *Geological Bulletin of China*, 21(12): 858-868 (in Chinese with English abstract)
- Pearce JA and Peate DW. 1995. Tectonic implications of the composition of volcanic Arc magmas. *Annual Review of Earth and Planetary Sciences*, 23: 251-285
- Qian Q, Gao J, Klemm R, He GQ, Song B, Liu DY and Xu RH. 2009. Early Paleozoic tectonic evolution of the Chinese South Tianshan Orogen: Constraints from SHRIMP zircon U-Pb geochronology and geochemistry of basaltic and dioritic rocks from Xiata, NW China. *International Journal of Earth Sciences*, 98(3): 551-569
- Rapp RP and Watson EB. 1995. Dehydration melting of metabasalt at 8-32 kbar: Implications for continental growth and crust-mantle recycling. *Journal of Petrology*, 36(4): 891-931
- Rushmer T. 1991. Partial melting of two amphibolites: Contrasting experimental results under fluid-absent conditions. *Contributions to Mineralogy and Petrology*, 107(1): 41-59
- Sun SS and McDonough WF. 1989. Chemical and isotopic systematics of oceanic basalts: Implications for mantle composition and processes. In: Saunders AD and Norry MJ (eds.). *Magmatism in the Ocean Basins*. Geological Society, London, Special Publication, 42(1): 313-345
- Tu XL, Zhang H, Deng WF, Ling MX, Liang HY, Liu Y and Sun WD. 2011. Application of RESolution in-situ laser ablation ICP-MS in trace element analyses. *Geochimica*, 40(1): 83-98 (in Chinese with English abstract)
- Wang B, Shu L, Faure M, Jahn BM, Cluzel D, Charvet J, Chung SL and Meffre S. 2011. Paleozoic tectonics of the southern Chinese Tianshan: Insights from structural, chronological and geochemical studies of the Heiyingshanophiolitic mélange (NW China). *Tectonophysics*, 497(1): 85-104
- Wang C, Luo JH, Che ZC, Liu L and Zhang JY. 2009. Geochemical characteristics and U-Pb LA-ICP-MS zircon dating of the Oxidaban pluton from Xinjiang, China: Implication for a Paleozoic oceanic subduction on process in southwestern Tianshan. *Acta Geologica Sinica*, 83(2): 272-283 (in Chinese with English abstract)
- Wang QH. 2007. Characteristics of structural deformation and its controlling factors of central and western segment in the front of the South Tianshan. Ph. D. Dissertation. Hangzhou: Zhejiang University, 1-164 (in Chinese with English summary)
- Wang RS, Wang Y, Li HM, Zhou DW and Wang JL. 1998. Zircon U-Pb age and its geological significance of high-pressure terrane of granulite facies in Yushugou area, southern Tianshan Mountain. *Geochemica*, 27(6): 517-522 (in Chinese with English abstract)
- Wolf MB and Wyllie PJ. 1994. Dehydration-melting of amphibolite at 10 kbar: The effects of temperature and time. *Contributions to Mineralogy and Petrology*, 115(4): 369-383
- Xia LQ, Xia ZC, Xu XY, Li XM, Ma ZP and Wang LS. 2007. *The Magmatism of Tianshan*. Beijing: Geological Publishing House, 1-350 (in Chinese)
- Xiao XC and Tang YQ. 1991. *Tectonic Evolution of Southern Margin for Paleo-Central Asia Complex Giant Suture*. Beijing: Science and Technology Publishing House, 1-240 (in Chinese)
- Xia XP, Sun M, Zhao GC, Li HM and Zhou MF. 2004. Spot zircon U-Pb isotope analysis by ICP-MS coupled with a frequency quintupled (213 nm) Nd-YAG laser system. *Geochemical Journal Japan*, 38(2): 191-200
- Xiao WJ, Huang BC, Han CM, Sun S and Li JL. 2010. A review of the western part of the Altaids: A key to understanding the architecture of accretionary orogens. *Gondwana Research*, 18(2): 253-273
- Xiao WJ, Windley BF, Allen MB and Han CM. 2013. Paleozoic multiple accretionary and collisional tectonics of the Chinese Tianshan orogenic collage. *Gondwana Research*, 23(4): 1316-1341
- Xu XY, Ma ZP, Xia ZC, Xia LY, Li XM and Wang LS. 2006. TIMS U-Pb isotopic dating and geochemical characteristics of Paleozoic granitic rocks from the middle-western section of Tianshan. *Northwestern Geology*, 39(1): 50-75 (in Chinese with English abstract)

- Xu XY, Wang HL, Li P, Chen JL, Ma ZP, Zhu T, Wang N and Dong YP. 2012. Geochemistry and geochronology of Paleozoic intrusions in the Nalati (Narati) area in western Tianshan, Xinjiang, China: Implications for Paleozoic tectonic evolution. *Journal of Asian Earth Sciences*, 72: 33–62
- Yang TN, Li JY, Sun GH and Wang YB. 2006. Earlier Devonian active continental arc in Central Tianshan: Evidence of geochemical analyses and zircon SHRIMP dating on mylonitized granitic rock. *Acta Petrologica Sinica*, 22(1): 41–48 (in Chinese with English abstract)
- Zhang CH, Zhou HR, Wang ZQ and Wang JS. 1998. Internal deformation of the nappes in the middle part of South Tianshan orogeny and its relationship to thrust structures. *Xinjiang Geology*, 16(4): 307–314 (in Chinese with English abstract)
- Zhang CL, Zhou DW, Wang JL and Wang RS. 2007. Geochronology, geochemistry and Sr-Nd isotopic composition and genesis implications of Huangjianshan granite intrusion in Kumishi area of southern Tianshan. *Acta Petrologica Sinica*, 23(8): 1821–1829 (in Chinese with English abstract)
- Zhou DW, Su L, Jian P, Wang RS, Liu XM and Wang JL. 2004. Zircon U-Pb SHRIMP ages of high-pressure granulite in Yushugou ophiolitic terrane in southern Tianshan and their tectonic implications. *Chinese Science Bulletin*, 49(14): 1411–1415 (in Chinese)
- Zhu YF, Zhang LF, Gu LB, Guo X and Zhou J. 2005. SHRIMP geochronology and geochemistry of Carboniferous volcanic rocks in the western Tianshan area. *Chinese Science Bulletin*, 50(18): 2004–2014 (in Chinese)
- Zhu ZX, Wang KZ, Zheng YJ, Sun GH, Zhang C and Li YP. 2006. Zircon SHRIMP dating of Silurian and Devonian granitic intrusions in the southern Yili block, Xinjiang and preliminary discussion on their tectonic setting. *Acta Petrologica Sinica*, 22(5): 1193–1200 (in Chinese with English abstract)
- Zhu ZX, Li JY, Dong LH, Wang KZ, Liu GZ, Li YP and Liu ZT. 2008. Age determination and geological significance of Devonian granitic intrusions in Seriyakeylake region, northern margin of Tarim basin, Xinjiang. *Acta Petrologica Sinica*, 24(5): 971–976 (in Chinese with English abstract)
- Zhu ZX, Li JY, Dong LH, Zhang XF, Wang KZ, Wang HX and Zhao TY. 2009. Tectonic framework and tectonic evolution of the southern Tianshan, Xinjiang, China. *Geological Bulletin of China*, 28(12): 1863–1870 (in Chinese with English abstract)
- Zuo GC and Li SX. 2011. Early Paleozoic tectonic framework and evolution in the northeast margin of Tarim basin. *Geology in China*, 38(4): 945–960 (in Chinese with English abstract)
- 李向东, 王庆明, 王克卓. 1998. 天山后碰撞阶段构造演化的新信息——来自阿吾拉勒山中段动力变质岩的证据. *地质论评*, 44(4): 443–448
- 李向东, 王克卓. 2000. 中国西天山南缘盆地构造转换解析. *新疆地质*, 18(3): 211–219
- 李向东, 肖文交, 周宗良. 2004. 南天山南缘晚泥盆世构造事件的⁴⁰Ar/³⁹Ar定年证据及其意义. *岩石学报*, 20(3): 691–696
- 李曰俊, 宋文杰, 买光荣, 周黎霞, 胡剑凤, 尚新路. 2001. 库车和北塔里木前陆盆地与南天山造山带的耦合关系. *新疆石油地质*, 22(5): 376–381
- 李曰俊, 王招明, 买光荣, 吴浩若, 黄智斌, 谭泽金. 2002. 塔里木盆地艾克提克群中放射虫化石及其意义. *新疆石油地质*, 23(6): 496–500
- 李曰俊, 杨海军, 赵岩, 罗俊成, 郑多明, 刘亚雷. 2009. 南天山区域大地构造与演化. *大地构造与成矿学*, 33(1): 94–104
- 刘颖, 刘海臣, 李献华. 1996. 用 ICP-MS 准确测定岩石样品中的 40 余种微量元素. *地球化学*, 25(6): 552–558
- 刘本培, 王自强, 张传恒. 1996. 西南天山构造格局与演化. 武汉: 中国地质大学出版社, 1–120
- 龙灵利, 高俊, 熊贤明, 钱青. 2007. 新疆中天山南缘比开(地区)花岗岩地球化学特征及年代学研究. *岩石学报*, 23(4): 719–732
- 毛景文, 韩春明, 王义天, 杨建民, 王志良. 2002. 中亚地区南天山大型金矿带的地质特征、成矿模型和勘查准则. *地质通报*, 21(12): 858–868
- 涂湘林, 张红, 邓文峰, 凌明星, 梁华英, 刘颖, 孙卫东. 2011. RESOLUTION 激光剥蚀系统在微量元素原位微区分析中的应用. *地球化学*, 40(1): 83–98
- 王超, 罗金海, 车自成, 刘良, 张敬艺. 2009. 新疆西达坂花岗岩体地球化学特征和锆石 LA-ICP-MS 定年: 西南天山古生代洋盆俯冲作用过程的启示. *地质学报*, 83(2): 272–283
- 王润三, 王焰, 李惠民, 周鼎武, 王居里. 1998. 南天山榆树沟高压麻粒岩地体锆石 U-Pb 定年及其地质意义. *地球化学*, 27(6): 517–522
- 王清华. 2007. 南天山南缘中西段构造变形特征与控制因素. 博士学位论文. 浙江: 浙江大学, 1–164
- 夏林圻, 夏祖春, 徐学义, 李向民, 马中平, 王立社. 2007. 天山岩浆作用. 北京: 地质出版社, 1–350
- 肖序常, 汤耀庆. 1991. 古中亚复合巨型缝合带南缘构造演化. 北京: 科学技术出版社, 1–240
- 徐学义, 马中平, 夏祖春, 夏林圻, 李向民, 王立社. 2006. 天山中西段古生代花岗岩 TIMS 法锆石 U-Pb 同位素定年及岩石地球化学特征研究. *西北地质*, 39(1): 50–75
- 杨天南, 李锦轶, 孙桂华, 王彦斌. 2006. 中天山早泥盆世陆弧: 来自花岗岩糜棱岩地球化学及 SHRIMP-U/Pb 定年的证据. *岩石学报*, 22(1): 41–48
- 张传恒, 周洪瑞, 王自强, 王家生. 1998. 南天山造山带中段推覆体内部变形及其与逆冲构造的关系. *新疆地质*, 16(4): 307–314
- 张成立, 周鼎武, 王居里, 王润三. 2007. 南天山库米什南黄尖石山岩体的年代学、地球化学和 Sr、Nd 同位素组成及其成因意义. *岩石学报*, 23(8): 1821–1829
- 周鼎武, 苏犁, 简平, 王润三, 柳小明, 陆关祥, 王居里. 2004. 南天

附中文参考文献

- 高俊, 张立飞, 刘圣伟. 2000. 西天山蓝片岩榴辉岩形成和抬升的⁴⁰Ar/³⁹Ar 年龄记录. *科学通报*, 45(1): 89–94
- 高俊, 龙灵利, 钱青, 黄德志, 苏文, Klemd R. 2006. 南天山: 晚古生代还是三叠纪碰撞造山带? *岩石学报*, 22(5): 1049–1061
- 高俊, 钱青, 龙灵利, 张喜, 李继磊, 苏文. 2009. 西天山的增生造山过程. *地质通报*, 28(12): 1804–1816
- 郭瑞清, 尼加提·阿布都逊, 秦切, 贾晓亮, 朱志新, 王克卓, 李亚萍. 2013. 新疆塔里木北缘志留纪花岗岩类侵入岩的地质特征及构造意义. *地质通报*, 32(2–3): 220–238
- 黄河. 2013. 中国南天山地区古生代花岗岩与区域地质演化. 博士学位论文. 北京: 中国地质大学, 1–144
- 姜常义, 穆艳梅, 赵晓宁, 白开寅, 张虹波. 2001. 塔里木板块北缘活动陆缘型侵入岩带的岩石学与地球化学. *中国区域地质*, 20(2): 158–163
- 李锦轶, 肖序常, 汤耀庆, 赵民, 冯益民, 朱宝清. 1992. 新疆北部金属矿产与板块构造. *新疆地质*, 10(2): 138–146

- 山榆树沟蛇绿岩地体中高压麻粒岩 SHRIMP 锆石 U-Pb 年龄及构造意义. 科学通报, 49(14): 1411 - 1415
- 朱永峰, 张立飞, 古丽冰, 郭璇, 周晶. 2005. 西天山石炭纪火山岩 SHRIMP 年代学及其微量元素地球化学研究. 科学通报, 50(18): 2004 - 2014
- 朱志新, 王克卓, 郑玉洁, 孙桂华, 张超, 李亚萍. 2006. 新疆伊犁地块南缘志留纪和泥盆纪花岗质侵入体锆石 SHRIMP 定年及其形成时构造背景的初步探讨. 岩石学报, 22(5): 1193 - 1200
- 朱志新, 李锦轶, 董连慧, 王克卓, 刘国忠, 李亚萍, 刘振涛. 2008. 新疆塔里木北缘色日牙克依拉克一带泥盆纪花岗质侵入体的确定及其地质意义. 岩石学报, 24(5): 971 - 976
- 朱志新, 李锦轶, 董连慧, 张晓帆, 王克卓, 王华星, 赵同阳. 2009. 新疆南天山构造格架及构造演化. 地质通报, 28(12): 1863 - 1870
- 左国朝, 李绍雄. 2011. 塔里木盆地东北缘早古生代构造格局及演化. 中国地质, 38(4): 945 - 960